Crosslinked isocyanate-free poly(hydroxy urethane)s – Poly(butyl methacrylate) hybrid latexes

Boris Bizet, Etienne Grau, Henri Cramail, José Maria Asua

Crosslinked Isocyanate-free Poly(Hydroxy Urethane)s – Poly(butyl methacrylate) Hybrid Latexes

Boris Bizet,[ab] Etienne Grau,[a] Henri Cramail[a] and José M. Asua*[b]*

[a] LCPO – UMR 5629, Université de Bordeaux – CNRS – Bordeaux INP, 16 Avenue Pey Berland Bât. A, 33607 Pessac, France

[b] POLYMAT, University of the Basque Country UPV/EHU, Joxe Mari Korta Center, Avenida Tolosa 72, 20018 Donostia-San Sebastián, Spain

KEYWORDS: Poly(Hydroxy)urethanes – PHUs, Bio-based Polymers, Crosslinking, PU-Acrylic Hybrid, Miniemulsion, Coatings

ABSTRACT

Waterborne isocyanate-free grafted poly(hydroxy urethane)-poly(butyl methacrylate) hybrid dispersions were synthesized by miniemulsion polymerization. Grafting was induced by including methacrylate functionalities in the poly(hydroxy urethane) and was controlled by the degree of functionalization. It is shown that grafting enabled a fine tuning of the mechanical properties of the PHU containing hybrids.

1. Introduction

Polymer-polymer hybrids are used to access materials that present superior performance due to the synergistic combination of the properties of the constitutive polymers.[1–4] Hybrid polyurethane-poly(meth)acrylic waterborne dispersions is one industrially relevant and environmentally benign example of these materials.[5] PUs provide the material superior mechanical properties such as toughness, flexibility and abrasion resistance[6–8] whereas the relatively low cost poly(meth)acrylics increases the outdoor and alkali resistance, as well as the pigment compatibility.[9–11] These dispersions find applications in areas such as adhesives[12–15] and/or coatings[16,17] as recently reviewed.[5] These hybrids can be prepared by blending of PU and poly(meth)acrylic dispersions.[18–22] However, blends yield films with poor mechanical properties because of the strong phase segregation. This problem is avoided by bi-phasic particles providing intimate contact between the two polymers,[16,17,29,21–28] which form films with better properties due to a more homogeneous distribution of the two polymers.

Mehravar *et al*. highlighted the challenge of reducing the environmental impact of the current industrial processes for the production of PU-(meth)acrylic hybrids (based on the use of isocyanates) by developing isocyanate-free synthetic methods.[5] The field of water-based non-isocyanate polyurethanes (NIPUs) has also been recently reviewed.[30] In contrast with classical PUs, the literature dealing with hybrid NIPU waterborne dispersions is very limited.[31–34] For the specific case of the NIPU-(meth)acrylic hybrids, only two studies have been reported where urethane functionalities are incorporated as pendant groups leading to a remarkable simultaneous increase of Young modulus, tensile strength and elongation at break.[31,32] In a previous article,[35] we developed a synthetic strategy to prepare waterborne poly(hydroxy urethane)s)/(meth)acrylic hybrids. Poly(hydroxy urethane)s – PHUs – a special class of NIPUs,

were first formed by bulk aminolysis of cyclic carbonates and a vegetable oil-based diamine (Priamine™ 1075) and then dissolved in butyl methacrylate (BMA). The resulting solution was then miniemulsified. The polymerization of BMA led to hybrid particles exhibiting a core-shell morphology with the PHU in the shell. The performance of these latexes revealed that the Young's modulus and stress at break decreased with the PHU content while the strain at break and the toughness showed a moderate increase. TEM and AFM images of the films showed that a substantial phase segregation occurred with the formation of large PHU domains, which reduced the interaction between the NIPU and the methacrylate, potentially limiting the properties achievable.

A way to avoid phase segregation is by grafting the PHU and the methacrylic polymer. This is an unexplored field and the results available for conventional PU-(meth)acrylate hybrids about the effect of grafting on the resulting performance (e.g. mechanical properties) are not particularly helpful as a guide because they are controversial. Thus, although there are many examples showing an improvement of the mechanical properties with grafting in terms of increased mechanical strength and Young's modulus,[23,36] there are also others where grafting has limited effect.[16,17,37]

Therefore, in this article, waterborne grafted PHU-poly(meth)acrylate hybrid dispersions were developed and the effect of grafting on the particle and film morphologies as well as on the mechanical properties of the films was investigated.

2. Experimental

2.1. **Materials.** Butyl acetate (BAc, > 99 %), butyl methacrylate (BMA, 99%), stearyl acrylate (SA, 97 %), tetrabutylammonium bromide (TBABr), glycidyl methacrylate (GMA, > 97

%), methacrylic anhydride (94 %) and *tert*-butyl hydroperoxide (TBHP, 70 % in water) were purchased from Sigma Aldrich; Sebacoyl Chloride (97 %) from Alfa Aesar; Glycerol 1,2-carbonate (90 %) from ABCR GmbH; Ascorbic acid (AsA, > 99.5 %) from Fluka; Hydrochloric acid (HCl) in isopropanol (0.1 mol.L^{-1}) from Panreac; Trimethylamine (NEt_3, 99 %) from Fisher; and Acetone was from VWR Chemicals. Silwet L-77® was purchased from Helena Chemical Company. Croda kindly provided Priamine™ 1075 (P1075). Dow Chemical kindly provided alkyl diphenyl oxide disulfonate (Dowfax™ 2A1, D2A1, 45 wt% in water). Deionized water was used throughout the work.

2.2. **Experimental design.** The synthesis of the waterborne grafted PHU-(meth)acrylic hybrids was carried out by dissolving PHUs containing methacrylic groups in a mixture of BMA and SA (the PHU was 20 wt% based on BMA, and SA was 4 wt% based on the total organic phase), dispersing the mixture in an aqueous solution of Dowfax 2A1 using sonication, and polymerizing the resulting miniemulsion employing a redox initiator system (TBHP/AsAc). Two different kinds of methacrylic functionalized PHUs were used.

In the first type, the methacrylic functionality was fixed at the PHU chain end. The synthesis is summarized in Scheme 1. The formulation used is given in Table S1 (Supporting Information). An amine-terminated PHU was synthesized by aminolysis between a sebacic acid-derived bis-cyclic carbonate (bisCC-C_{10}) and an excess of the commercially available Priamine™ 1075 (P1075). The excess of diamine was chosen to target a degree of polymerization of 10. The reaction was performed without catalyst for 4 h at 90°C in bulk in a Schlenk tube using a helical stirrer specifically designed to fit in the Schlenk vessel (Step #1). The amount of NH_2-moieties was measured by titration with HCl in isopropanol. The amine-terminated PHU was then reacted

with the equimolecular amount of mono-carbonate derivative of glycidyl methacrylate (monoCC-GMA) at 90 ºC for 20h (Step #2). bisCC-C_{10} was synthesized according to the procedure described in our previous article.[35] No purification of the functionalized PHUs was performed after reaction.

The second type of methacrylic-functionalized PHUs contained the methacrylic groups distributed along the PHU chain and was synthesized as depicted in Scheme 2. The formulation used is given in Table S2 (Supporting Information). The amine functionalized PHU was prepared by aminolysis between bisCC-C_{10} and P1075 as described above. Then, methacrylic anhydride was added and the system was kept for 20h at 90°C. The amount of methacrylic anhydride was half of the theoretical amount of OH-moieties produced during PHU synthesis (assuming complete conversion of the cyclic carbonate groups). No purification of the functionalized PHUs was performed after reaction.

The monoCC-GMA was synthesized by reacting glycidyl methacrylate (GMA) with carbon dioxide (CO_2) in acetone under pressure using tetrabutylammonium bromide (TBABr) as catalyst – Scheme 3. 9.5 g (66.83 mmol) of glycidyl methacrylate and 0.285 g (0.88 mmol) of tetrabutylammonium bromide (TBABr) were mixed together and dissolved in 50 mL acetone. The mixture was maintained at 80°C under 30 bars of CO_2 and mechanical stirring during 5 days. Full conversion was obtained according to ^{1}H-NMR analysis Figure S1 (Supporting Information). Removal of the acetone solvent under reduced pressure allowed recovering the final product that was utilized without any further purification.

For the sake of comparison, a non-functionalized poly(hydroxy urethane) was synthesized by aminolysis reaction between bisCC-C_{10} and P1075 using a stoichiometric ratio for the reactive

moieties.[35] No catalyst was added for the polymerization reactions and no purification of the PHUs was performed after reaction. (The molar masses measured by SEC in DMF – PS calibration – were: $\bar{M}_n$ = 2,2.10^4 g.mol^{-1} and Đ = 1.9).

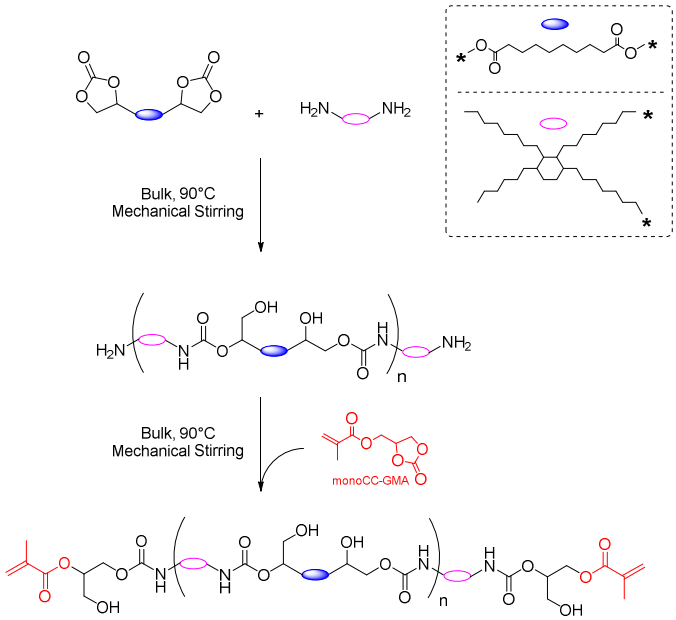

Scheme 1: 1 pot – 2 step synthesis of the methacrylate-terminated poly(hydroxy urethane)s

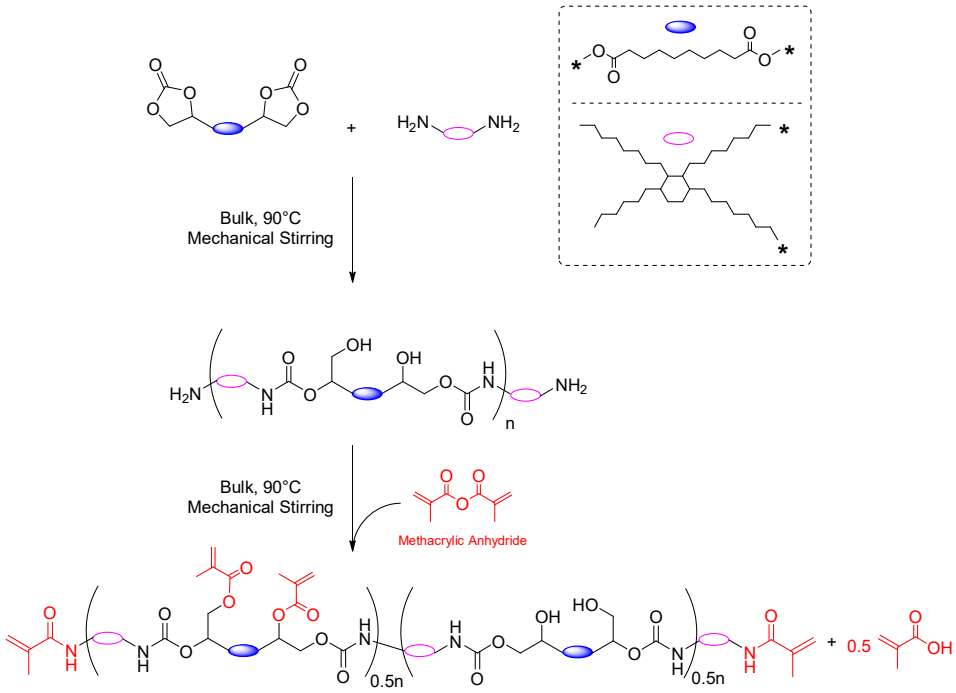

Scheme 2: Synthesis of reactive PHUs containing methacrylic groups along the chain (50% functionalization)

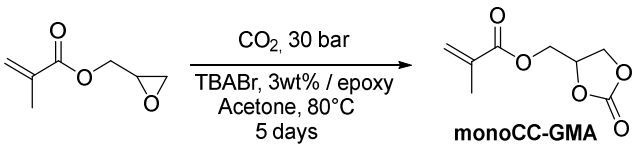

Scheme 3: Carbonation reaction of glycidyl methacrylate to its corresponding mono-cyclic carbonate (monoCC-GMA)

The formulations used for the synthesis of the waterborne PHU-(meth)acrylates hybrids by miniemulsion polymerization are summarized in Table 1 and further details are given in the Supporting Information (Table S3). In order to prepare the miniemulsion, the functionalized PHUs (20 wt% based on BMA) were dissolved in a mixture of BMA and SA (SA being 4 wt% based on organic phase) at 80°C. The organic phase was added dropwise to an aqueous solution of Dowfax 2A1 (1 wt% based on organic phase) in deionized water under vigorous magnetic

stirring. The resulting 40 wt% solids content coarse emulsion was sonicated for 30 min in a Hielscher Ultrasonics GmbH (ref UIS250V; 100% amplitude, 0.8s duty cycle). After miniemulsification, another 1 wt% (based on organic phase) of Dowfax 2A1 was added to the miniemulsion. The reason for this post-stabilization step is that for this system, the droplet size was controlled by the available surfactant and therefore the droplets were sparingly covered by the surfactant, namely close to the stability limit.[38,39] The resulting miniemulsion was transferred into a 3-neck round-bottom flask. An aqueous solution of TBHP was then added as a shot so that it had enough time to partition between the aqueous and the organic phase. After the nitrogen flushing (at least 50 min at 70°C), an aqueous solution of AsAc was fed during 2.5h. Note that TBHP does not suffer any significant decomposition at 70°C.[40]

The reaction mixture was left under magnetic stirring at 70°C during the entire period of feeding. Regular sampling was performed in order to gauge the conversion (by gravimetry) and the particle size (by DLS). At the end of the process, the latex was cooled down to room temperature and filtered through a 85 µm mesh in order to collect and measure the amount of formed coagulum (if any).

Table 1: Formulations used in the miniemulsion polymerizations (details in Table S3)

		Composition			
Basic recipe	PHU	20	wt%	96wt%	40 wt% solids
	BMA	80	wt%		
	SA	4	wt%		
	Dowfax™ 2A1	1	wt% (wbo)		
	Water				
Post-Stabilization	Dowfax™ 2A1	1	wt% (wbo)		
	Water	< 1g			
Initiation	TBHP	0.1	wt% (wbo)		
	AsAc	0.1	wt% (wbo)		
	Water	<1g			

2.3. **Film casting.** Films were cast from the latexes in silicone molds. A 1 wt% of wetting agent (Silwet L-77®) was used to reduce the surface tension of the dispersion allowing good wetting of the silicone. The wetting agent may also plasticize the polymer, and hence affect the mechanical properties of the film, but will not interfere in the comparison between the different polymers. Rectangular specimens were cast for tensile tests (10 x 40 x 0.3 mm^3) at 30°C, 55% relative humidity for 48h. Square samples were cast for TEM (10 x 10 x 0.5 mm^3) at RT, 55% relative humidity for 48h. These samples were cut with a cryo-microtome device.

2.4. **Characterization.** A Bruker Avance 400 spectrometer (400.20 MHz or 400.33 MHz) was used to record ^{1}H-NMR spectra. The samples were dissolved in DMSO-d6 at room temperature for the analyses. The conversion of the carbonate was calculated using Eq. 1 from the integrals of the CH_2 in alpha-position of the urethane moiety (δ = 2.9 ppm) and of the quaternary carbon of the bis-cyclic carbonate monomers (δ = 5 ppm).

$$\text{Conversion (\%)}_{\text{carb}} = \frac{\frac{\int \text{Urethane}_{(\delta_{\text{ppm}} = 2.9)}}{2}}{\frac{\int \text{Urethane}_{(\delta_{\text{ppm}} = 2.9)}}{2} + \int \text{Carbonate}_{(\delta_{\text{ppm}}=5)}} \quad (1)$$

The urethane : urea : amide ratio was calculated according to the integrals of the labile protons using the following equations:

$$\%_{\text{Urethane}} = \frac{\int \text{Urethane}_{(\delta_{\text{ppm}} = 7.1)}}{\int \text{Urethane}_{(\delta_{\text{ppm}} = 7.1)} + \int \text{Amide}_{(\delta_{\text{ppm}} = 7.7)} + \frac{\int \text{Urea}_{(\delta_{\text{ppm}} = 6.8)}}{2}} \quad (2)$$

$$\%_{\text{Amide}} = \frac{\int \text{Amide}_{(\delta_{\text{ppm}} = 7.7)}}{\int \text{Urethane}_{(\delta_{\text{ppm}} = 7.1)} + \int \text{Amide}_{(\delta_{\text{ppm}} = 7.7)} + \frac{\int \text{Urea}_{(\delta_{\text{ppm}} = 6.8)}}{2}} \quad (3)$$

$$\%_{\text{Urea}} = 1 - \%_{\text{Urethane}} - \%_{\text{Amide}} \quad (4)$$

Dynamic light scattering (DLS) measurements were performed in a Zetasizer Nano Z (Malvern Instruments). The reported values are the average of three repeated measurements of the z-average values, measured at 25°C after 15 sec equilibration time, of a sample of the latex that had previously been diluted in deionized water.

Size Exclusion Chromatography (SEC) in dimethylformamide (DMF with 1 g/L of LiBr salt) was used to measure the PHUs' molar masses. The equipment was composed of an Ultimate 3000 system from Thermoscientific equipped with diode array detector. A differential refractive index detector (dRI) from Wyatt technology was also part of the equipment. Two KD803 Shodex gel columns and one KD804 Shodex gel columns (300 x 8 mm) (exclusion limits from 1000 Da to 700 000 Da) were used. The flowrate was 0.8 mL min^{-1} and the temperature 50°C. Polystyrene standards (Easivial kit from Agilent) were used, with M_ns ranging from 162 to 364 000 Da.

Regarding the hybrids, the molar mass distribution of the whole polymer was measured by asymmetric-flow field-flow fractionation (AF4, Wyatt Eclipse 3) with multiangle Laser light scattering (MALLS) and refractive index (RI) detectors and using THF as the solvent. The setup consisted of a pump (LC-20, Shimadzu) coupled to a DAWN Heleos multiangle light scattering laser photometer (MALS, Wyatt) equipped with a He–Ne laser (λ = 658 nm) and an Optilab Rex differential refractometer (λ = 658 nm) (RI, Wyatt Technology). In AF4, the separation is based on the interplay between the flows of the carrier and the Brownian motion of the macromolecules occurring in an open channel in which one of the walls is a membrane.[41] The sample is first fixed against the membrane using a cross-flow. The interplay between the cross-

flow and the diffusion creates a profile of macromolecular sizes such as the large sizes are closer to the membrane wall. The parabolic flow along the cell makes that the macromolecules that are further away from the membrane (*i.e.*, the smaller ones) are eluted first. The main advantage of AF4 is that, due to the lack of stationary phase, very large macromolecules can be analyzed. The data collection and treatment were carried out by ASTRA 6 software (Wyatt Technology). The samples were prepared by dispersing the latexes directly in THF (5 mg of polymer latex in 1 mL of THF).[15] The molar mass was calculated from the RI/MALLS data using the Debye plot (with second-order Berry formalism).

Titration of the excess of NH_2-moieties (chain-ends) was performed with HCl in isopropanol, using bromocresol green as a color indicator. The reported values are an average of 3 replicates.

Transmission electron microscopy (TEM) was used in order to study the particle and film morphologies. The device was a TECNAI G^2 20 TWIN microscope operated at 200 kV and equipped with LaB6 filament, and high angle annular dark-field-scanning transmission electron microscopy (HAADF-STEM). Phosphotungstic acid was used as a staining agent for the particles and ultra-thin sections of the films (about 80 nm) were analyzed without any staining.

Differential Scanning Calorimetry (DSC) thermograms were measured using a DSC Q100 apparatus from TA Instruments. For each film sample, the following temperature program was applied: from -80°C to 130°C at 10°C min^{-1} and from 130°C to -80°C at 10°C min^{-1}. The glass transition temperatures (T_gs) were calculated from the first heating ramp so that the properties of the films after casting are obtained.

The minimum film formation temperature (MFFT) was measured by applying a thin layer of latex (60 µm thickness) onto a steel bar with a temperature gradient. After the water evaporated

and the film formed, thermocouples located at regular distances allowed for the measurement of the MFFT, which was defined as the temperature at which both a clear coat was observed and a clear cut could be made with a knife without formation of powder.

Tensile stress-strain measurements were carried out from the cast rectangular films (10 x 40 x 0.3 mm^3) with a texture analyzer (Stable Micro Systems Ltd., Godalming, UK). The reported results were the average of at least 3 different specimens measured at a constant velocity of 0.42 $mm.s^{-1}$. The Young's modulus was determined as the slope of the stress-strain curve before the yield point (elastic region) and the toughness was determined as the area under the obtained curve.

The gel content was measured gravimetrically after 24 h of Soxhlet extraction in technical-grade tetrahydrofuran (THF) according to previously reported method.[16]

3. Results and Discussion

3.1. Synthesis of the functionalized PHUs

Bi-functional methacrylate-terminated PHU.

The synthesis of a methacrylate-terminated PHU was performed as described in Scheme 1. Some of its characteristics are given in Table 2. Step #1 corresponded to the formation of the NH_2-terminated PHU by reaction of bisCC-C_{10} and P1075 and Step #2 is the functionalization of the NH_2-terminated PHU with monoCC-GMA. Both reactions were carried out in bulk. It can be seen that the measured molar mass was higher than that targeted. For the SEC, this was likely due to the use of PS standards. In the case of the degree of polymerization obtained from the titration of the amine groups, the even higher value found was likely due to the reaction between

NH_2 groups and the urethane and/or the ester moieties of the PHU backbone that resulted in a consumption of amine groups (Scheme S1). Actually, the resulting urea and amide groups were detected by ^{1}H-NMR, (Figure 1 and Table 2).

Table 2: Characteristics of the bi-functional, methacrylate-terminated PHU

Run	Targeted DP[a]	Reaction Step	Reaction Time	Conversion[b]		Amide : Urea : Urethane Ratio[e]	M_n[f] [g.mol]	Đ[f]	Titration[g]		
				U[c]	F[d]				$[NH_2]_{app}$ [mol.g^{-1}]	Mn_{app} [g.mol^{-1}]	DP_{app}
Bi-functional	10	#1	4h	n.d.	-	25 : 13 : 65	11600	1.8	$1.51.10^{-4}$	13350	28
		#2	20h	66%	60%	18 : 17 : 65	13400	1.9	$2.42.10^{-5}$	-	-

[a] Calculated according to Carother's theory
[b] Calculated *via* ^{1}H-NMR
[c] Conversion of the carbonate moiety into urethane
[d] Conversion of the methacrylic protons of monoCC-GMA into methacrylic protons attached to the PHU backbone
[e] Calculated from the labile proton zone
[f] SEC performed in DMF with LiBr salts. PS standards.
[g] Performed with HCl in isopropanol with bromocresol green as indicator
n.d. not determined

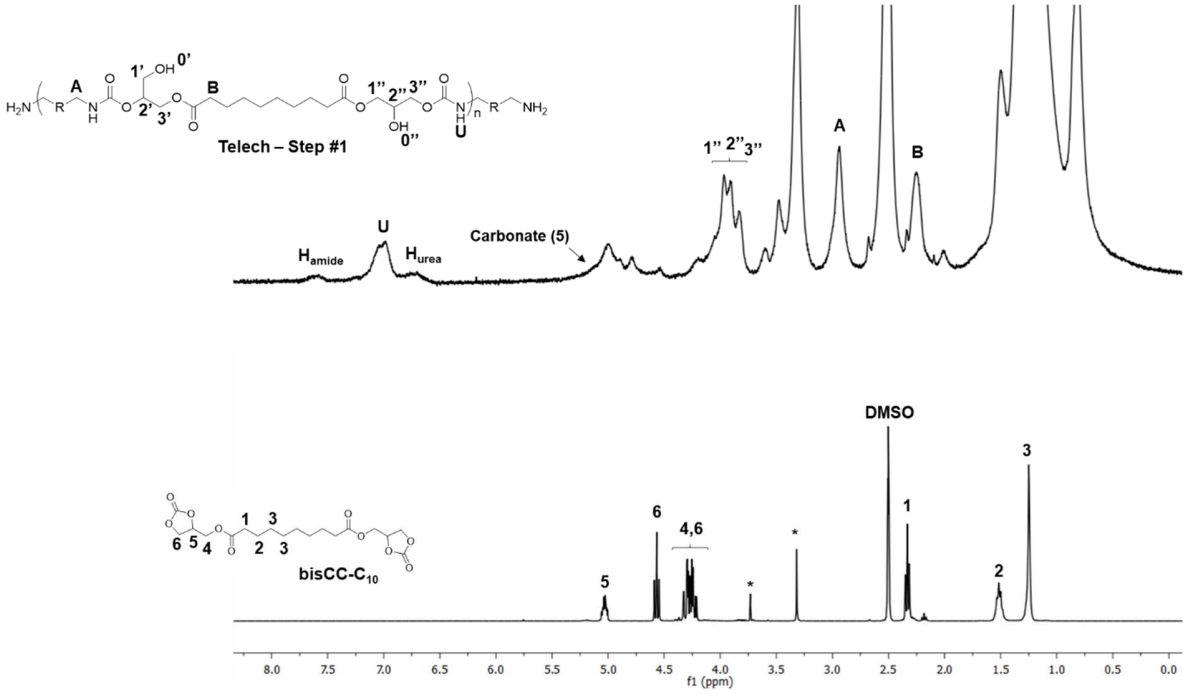

Figure 1: Stacked ^{1}H-NMR Spectra of bisCC-C_{10} and the NH_2-terminated PHU (Telech – Step #1) in DMSO-d6.

The amine-terminated PHU was then functionalized with monoCC-GMA. The shifts of the peaks corresponding to the acrylic protons at 5.68 and 6.06 ppm (noted F2 in Figure 2) in the ^{1}H-NMR spectra confirmed the incorporation of monoCC-GMA. In addition, no NH_2 moieties were detected when the resulting methacrylic-functionalized PHU was titrated with HCl in isopropanol.

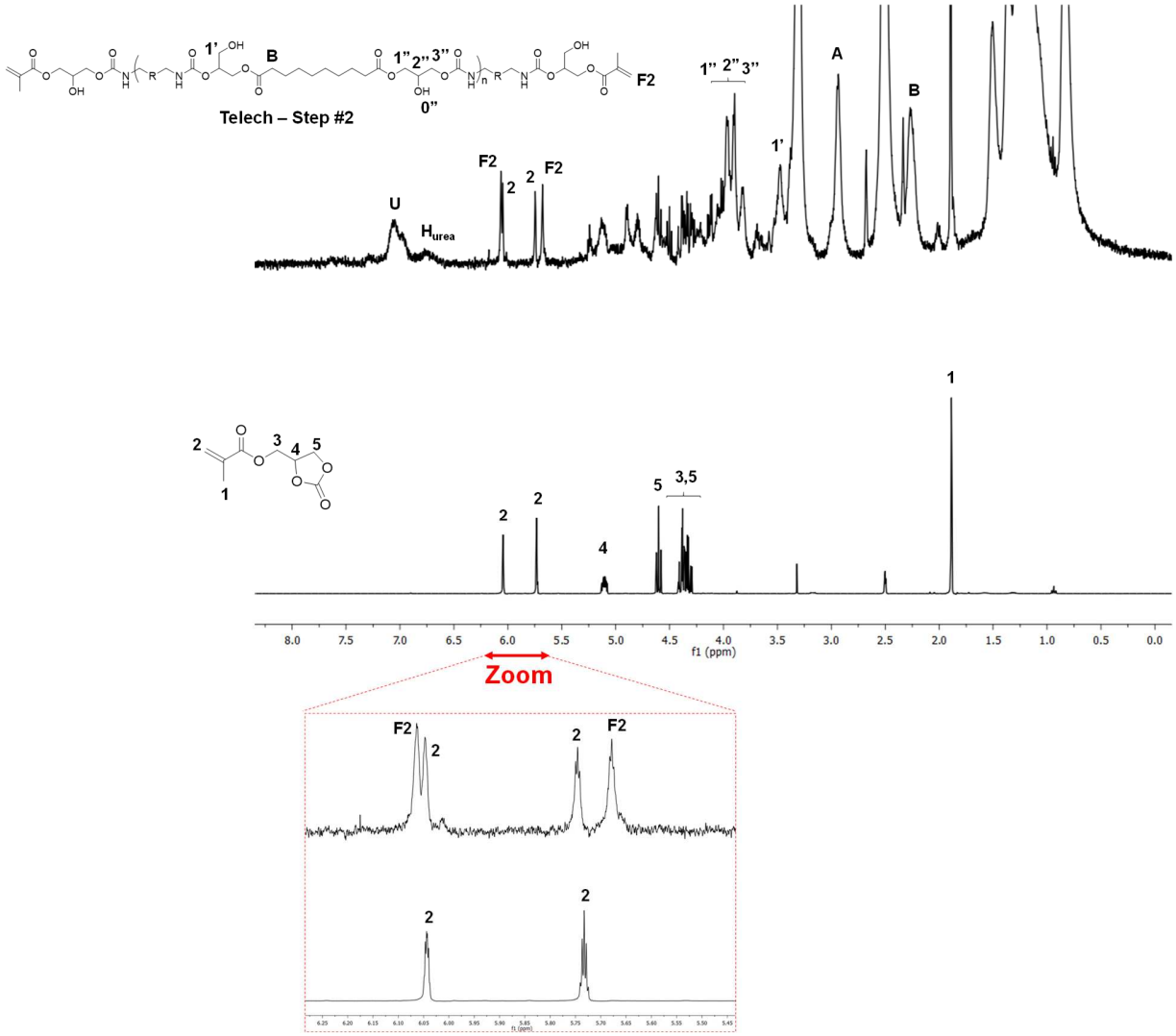

Figure 2: Stacked ^{1}H-NMR Spectra of monoCC-GMA and the methacrylic-terminated PHU (Telech – Step #2) in DMSO-d6.

Multi-functionalized PHU. Methacrylate groups were grafted along the PHU chain by reacting the OH-groups of the PHUs with methacrylic anhydride using the formulation in Table S2 (Scheme 2). The amount of added methacrylic anhydride was adjusted so that 50% of the theoretical amount of hydroxyl moieties got functionalized. The resulting ^{1}H-NMRs are shown in Figure 3 and some characteristics of the multi-functionalized PHU are listed in Table 3. The

peak at 2.9 ppm in the ^{1}H-NMR spectrum of the NH_2-terminated PHU pre-polymer confirmed the formation of the urethane moiety. However, some characteristic peaks of the PHUs such as the one corresponding to the CH_2 moiety in alpha position of the ester-groups of the bisCC-C_{10} (usually showing at chemical shifts closed to 2.1-2.2 ppm) could not be observed. This was due to a poor solubility of the sample in DMSO-d6 and in DMF, since small white agglomerates could be observed. Nevertheless, after functionalization with methacrylic anhydride, no problems of solubility were observed and the cyclic carbonate moiety could be clearly observed (around 5 ppm), allowing for the calculation of the conversion. For the peak assignments of the methacrylate multi-functionalized PHUs, we followed the recent work of Mülhaupt and coworkers.[42] The peaks of the methacrylic protons (peaks F2 at 5.61 and 5.98 ppm, zoom in Figure 3) appeared at higher chemical shifts than the ones of methacrylic acid. From these peaks it was calculated that about 60% of the methacrylic anhydride reacted with pendant OH-groups of the PHU backbone. Therefore, about 30% of the pendant OH-groups were substituted. The peak at 5.28 ppm (F3) was attributed to the quaternary proton attached to the functionalized pendant OH-groups. All these informations indicated that the PHU was functionalized with methacrylic groups in the backbone. Moreover, labile protons of amide and urea moieties could be noticed, suggesting the occurrence of side-reactions as described above. Finally, it was surprising to observe the appearance of a broad peak at 7.83 ppm (circled in red in Figure 3), that could unfortunately not be identified. Because of its proximity with the amide labile proton, it could be assumed that NH_2 moieties (from free P1075 or NH_2-terminated growing chains of PHU) reacted with methacrylic anhydride to form the corresponding amide, following a similar mechanism to the one described in Scheme S1, but no further investigation was performed.

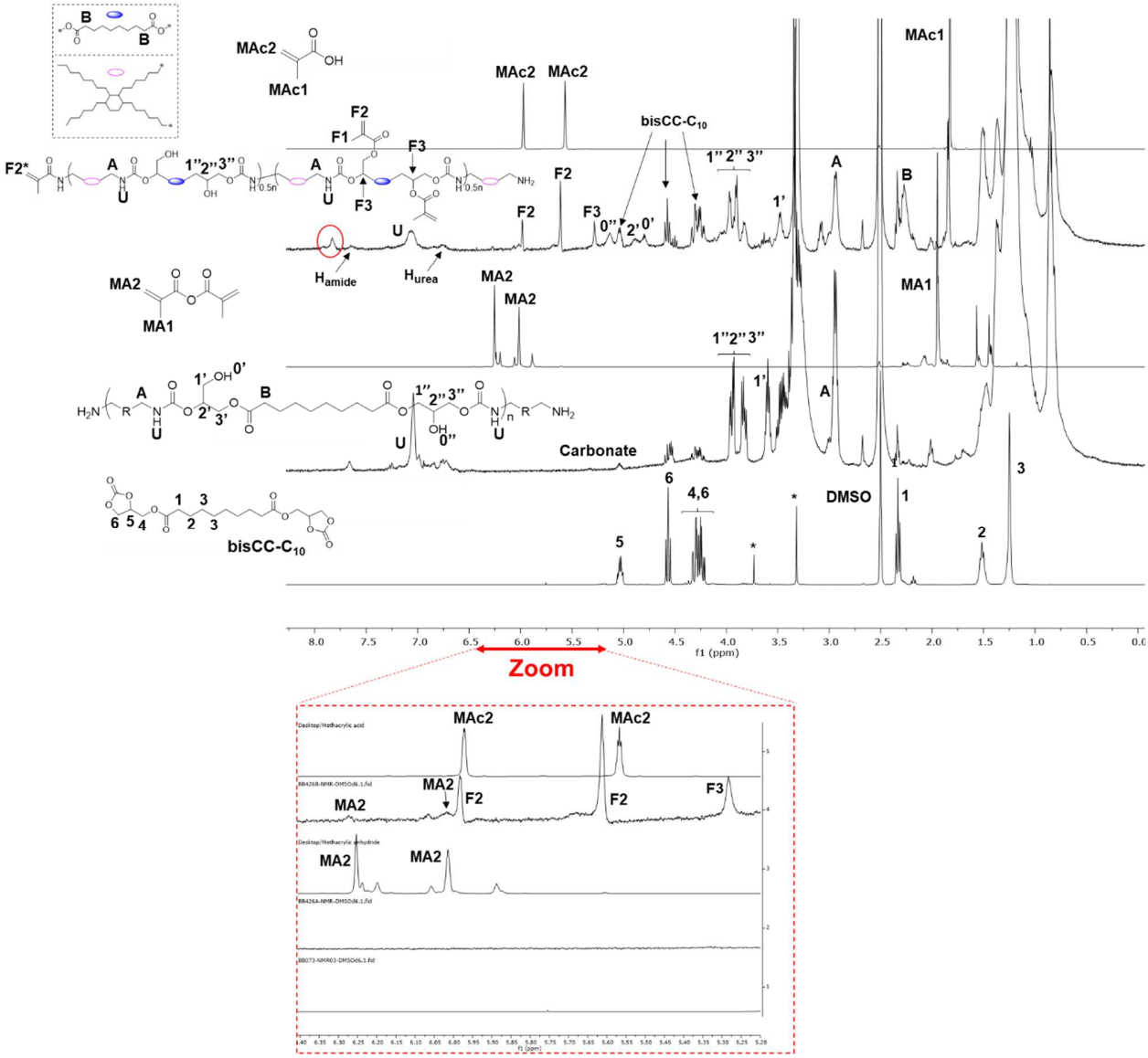

Figure 3: ^{1}H-NMR spectra of bisCC-C_{10}, the NH_2-terminated PHU from Step 1, methacrylic Anhydride, the multi-functionalized PHU from Step 2 and methacrylic Acid (from bottom to top) in DMSO-d6

Table 3: Characteristics of the multi-functionalized radical-reactive PHU pre-polymer

Run	Targeted DP[a]	Reaction Step	Reaction Time	Conversion[b]		Amide : Urea : Urethane Ratio[e]	M_n[f] [g.mol]	Đ[f]
				Ureth[c]	Meth[d]			
Multi-functional	10	#1	4h	n.d.	-	n.d.	4100 *	1.1*
		#2	20h	66%	60%	19 : 19 : 62	7500	1.4

[a] Calculated according to Carother's theory
[b] Calculated *via* ^{1}H-NMR
[c] Conversion of the carbonate moiety into urethane
[d] Conversion of methacrylic protons of monoCC-GMA into methacrylic protons attached to the PHU backbone
[e] Calculated from the labile proton zone in ^{1}H-NMR
[f] SEC performed in DMF with LiBr salts (PS calibration)
[g] Performed with HCl in isopropanol with bromocresol green as indicator
* An insoluble fraction in DMF was noticed
n.d. not determined

3.2. Synthesis of the hybrid latexes

The hybrid latexes were prepared by miniemulsion polymerization. 40 wt% solids content miniemulsions containing butyl methacrylate (BMA), stearyl acrylate (SA) (4 wt% of organic phase) and PHU (20 wt% based on BMA) were prepared as detailed in the experimental section. The free radical polymerization was initiated with the *tert*-butyl hydroperoxide / ascorbic acid (TBHP/AsAc) redox pair. TBHP was in the initial charge and AsAc was fed during 2.5 h.

Figure 4 presents the evolution of the gravimetric BMA conversion for the miniemulsion polymerizations carried out with the two methacrylic functionalized PHUs. It can be seen that induction periods were observed because the radicals initially formed upon feeding of AsAc were consumed by the inhibitor contained in the monomers (notice that monomers of technical

grade were used). The multi-functionalized PHU presented a shorter inhibition period (discussed below). Conversions approaching 100% at the end of the process were obtained.

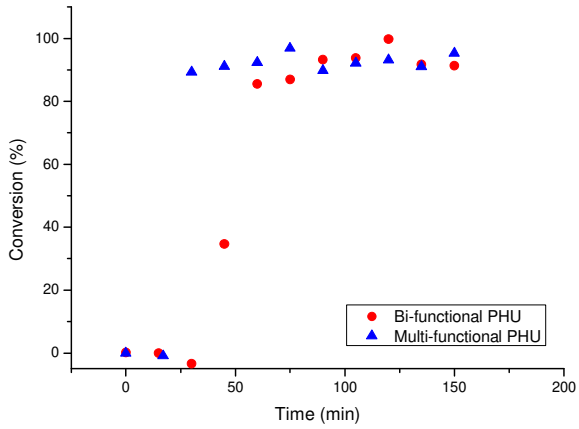

Figure 4: Conversion of BMA obtained by gravimetry upon polymerization with different functionalized PHUs: a) bi-functional, b) multi-functional PHU.

Figure 5 depicts the evolution of the particle size (z-average) and the number of particles per liter during polymerization. The number of particles was calculated from the measured diameter by DLS. It can be seen that the number of particles remained constant during the whole process, which indicates an efficient nucleation of the miniemulsion droplets and an absence of significant secondary nucleation. On the other hand, much lower particle diameters were obtained in the case of the multi-functionalized PHUs than for bi-functionalized PHUs. This can be explained by the presence of methacrylic acid that was formed upon functionalization and not removed before dissolving the reactive PHU into BMA. The methacrylic acid increased the hydrophilicity and the charge density on the surface of the particles increased, resulting in a decrease in the particle diameter. The higher number of particles resulted in a shorter inhibition period.

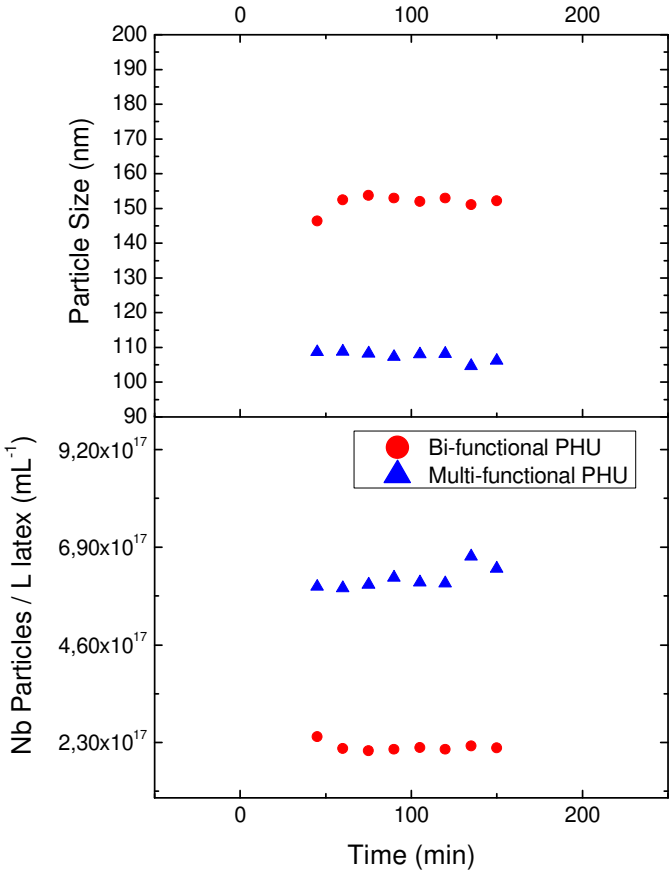

Figure 5: Evolution of the particle size and of the number of particles upon free radical polymerization of cross-linked H-NIPUs

The characteristics of the synthesized latexes are listed in Table 4. For comparison purposes, this Table also includes the latex synthesized with a non-functionalized PHU,[35] although it should be kept in mind that the comparison is not straightforward as the concentration of initiator was lower in this experiment. Asymmetric flow field flow fractionation (AF4) was utilized in order to measure the molar mass of the obtained products. AF4 uses an open channel for separation and therefore large molar masses and even cross-linked particles can be measured. The AF4 traces for RI and LS detectors and the molar mass distributions are given in Figure 6. It is worth

pointing out that the response of the LS detector is more sensitive to higher molar masses, and therefore the LS and RI traces are different. Actually, for the present case, the low molar mass peak was not detected by the LS detector. It can be seen that the RI trace for the non-functionalized PHU showed two peaks. The small one corresponded to the PHU (values in italics in Table 4) and the large one to poly(butyl methacrylate). The relative mass of the two peaks is close to 1/5, which corresponds to the weight fraction between PHU and (meth)acrylate monomers used in the formulation.

The RI trace of the bi-functionalized PHU presented two peaks clearly indicating that there was some PHU that was not grafted to the (meth)acrylic polymer. A 65% grafted fraction of PHU was estimated from the areas of the two peaks. Possible reasons for the limited grafting are the existence of a fraction of non-functionalized PHU and/or the slower reactivity of the telechelic methacrylic groups (it is known that macromonomers are less reactive than regular monomers).[43,44] Figure 6 also presents the molar mass distribution. It can be seen that the molar masses were in the range of 7.10^8 $g.mol^{-1}$, which is about 30% smaller than the size of the polymer particle (about 150 nm), suggesting that a large portion of the polymer in the particles formed a single cross-linked macromolecule. This is supported by the high gel fraction (84%) determined by Soxhlet extraction. This indicated that a substantial part of the functionalized PHU was really bi-functionalized.

The RI trace of the multifuctionalized PHU did not present any residue of ungrafted PHU (Figure 6c) showing a complete incorporation of the PHU into the (meth)acrylic polymer. In addition, a high gel content (84%) was determined by Sohxlet extraction in THF. The molar mass was about 4.10^8 $g.mol^{-1}$, which corresponded well with the size of the particles (106 nm in Table 4). Comparison with the bifunctional PHU suggested a stronger grafting for the

multifunctional PHU. This hypothesis is supported by the shift of the T_g of the PHU towards higher temperatures (see below in Figure 8).

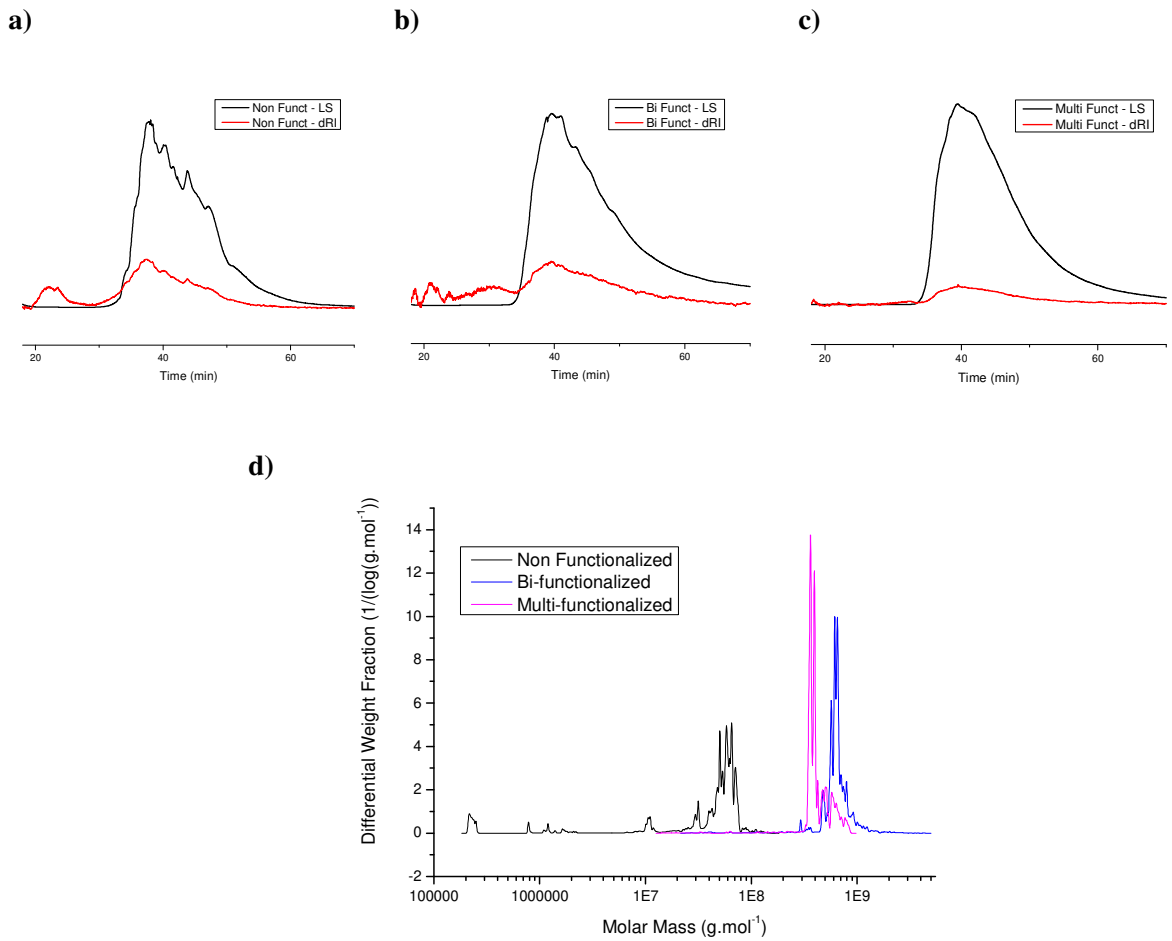

Figure 6: AF4 traces of the latexes (a) non-functionalized PHU, b) bi-functionalized PHU and c) multi-functionalized PHU) and d) Molar Mass Distributions as obtained by means of AF4

Table 4: Characteristics of the synthesized latexes (20 wt% NIPU, 2h30 feeding)

Type of reactive PHU	Coagulation [wt%]	Particle Size[a] [nm]	M_ns[b] [g.mol^{-1}]	M_ws[b] [g.mol^{-1}]	Đ[b]	Gel Content [%][c]	T_gs[d] [°C]	MFFT [°C]
Non-functionalized[e]	2.1	138	*4.1.10^4* 1.7.10^7	*7.2.10^4* 5.0.10^7	*1.8* 3.0	0	-20/27	15
Bi-functionalized	2.2	152	5.0.10^8	6.6.10^8	1.3	84	-13/26	18
Multi-functionalized	2	106	3.6.10^8	4.3.10^8	1.2	84	-12/26	27

[a] Measured by DLS

[b] Determined by AF4 (Asymmetric Flow Field Flow Fractionation). For the non-functionalized PHU, M_ns and M_ws for the PHU (italics) and for the polymethacrylate are given.
[c] Measured by Soxhlet extraction of the latexes
[d] Measured by DSC of the dried films
[e] Non-crosslinked latex, 20wt% PHU, fed during 2h30 with AsAc
- not determined because of a too low LS signal

An attempt to determine the morphology of the hybrid particles was carried out by means of TEM using phosphotungstic as staining agent. The resulting pictures are provided in Figure 7. No evidence of presence of different phases could be observed. However, this does not mean that the particles were homogeneous due to grafting as the particles looked homogeneous even with the non-functionalized PHU. The reason was that the amount of PHU (20 wt%) was not enough to see the PHU that was located at the surface of the particle (in a particle of 150 nm, 20% of the matter corresponds to a 5 nm thick shell). On the other hand, the TEM analyses confirmed the particle sizes observed by DLS, with much smaller particle diameters for the multifunctional PHU.

3.3. Film properties

Clear films were prepared at room temperature (Figure S3). Table 4 shows that the minimum film forming temperature (MFFT) increased with the crosslinking density. The effect of the polymer structure was also observed in the T_gs (Figure 8). All the hybrids presented two T_gs, one corresponding to the (meth)acrylic polymer and another one to the PHU. However, whereas the T_g of the (meth)acrylic part was roughly unaffected (about 26-27°C), that of the PHU varied from -20°C for the non-functionalized to -12°C for the multifunctionalized one, which is a strong proof of grafting.

Therefore, the increase in MFFT with the extent of grafting/crosslinking can be attributed to the decrease of the fraction of free soft PHU and the stronger mechanical properties of the crosslinked particles.

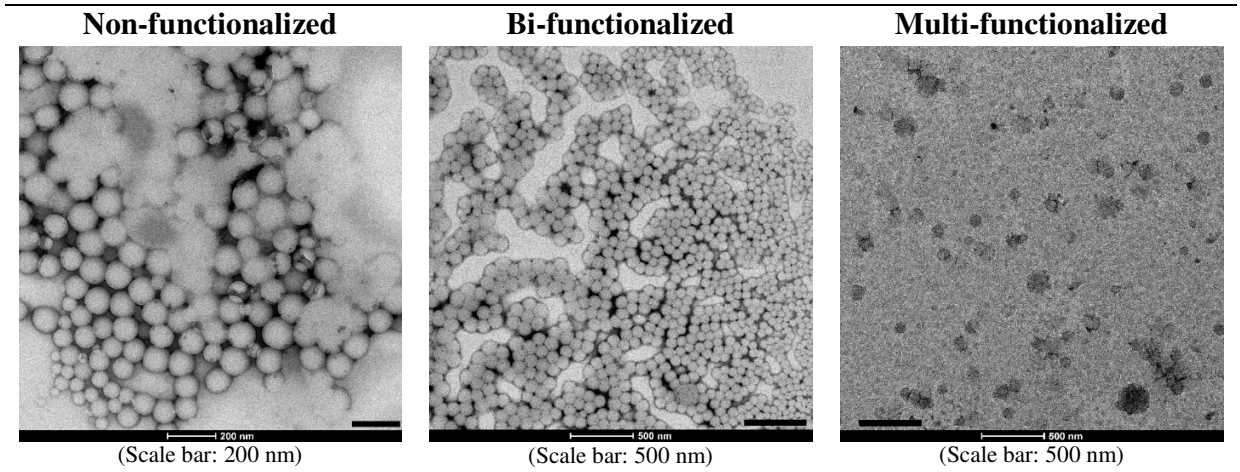

Figure 7: TEM images of the hybrid particles.

In order to shed some light on these results, the morphology of the films cast at room temperature and 55% relative humidity was studied. Figure 9 presents the TEM images of the cross-sections of the films. It can be seen that in the film containing the bi-functional PHU, the presence of particles with a core-shell morphology was evident. The dark phase was attributed to be PHU, as it was shown in a previous study,[35] that for PHU-polyBMA hybrids, PHU clusters appeared darker. This kind of particles could also been seen in the case of the multi-functionalized PHU, although in this case, they are not as evident, in part due to the smaller particle size.

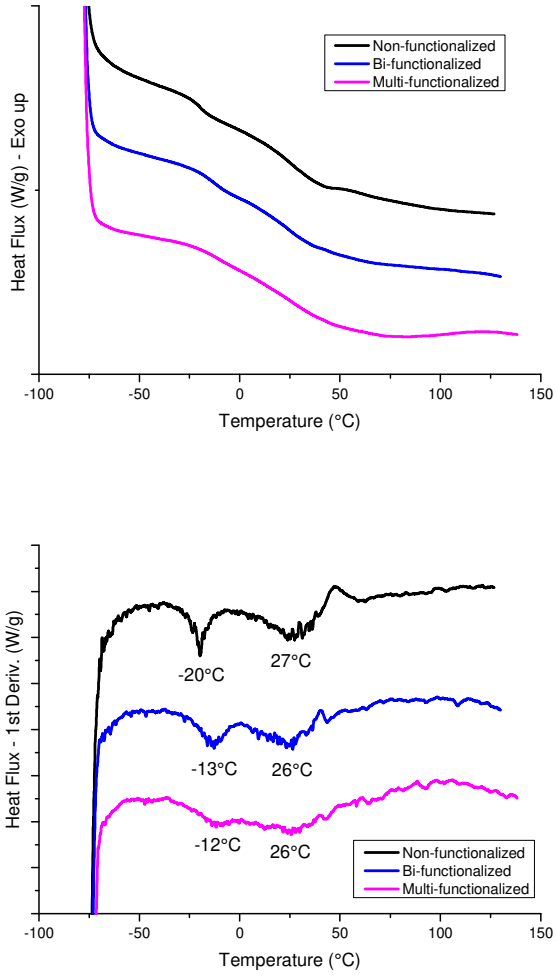

Figure 8: DSC curves of the cast films (top) and their first derivatives (bottom) depending on the chemical composition (1st heating ramp – 10°C/min)

Non-functionalized	Bi-functionalized	Multi-functionalized
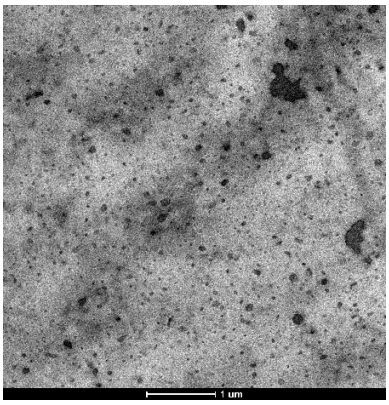	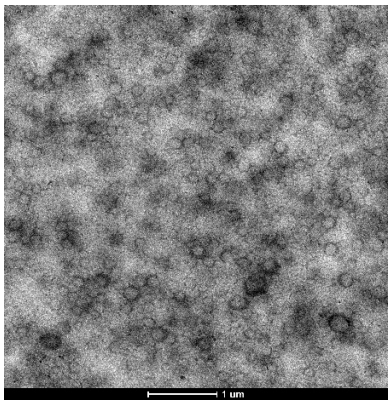	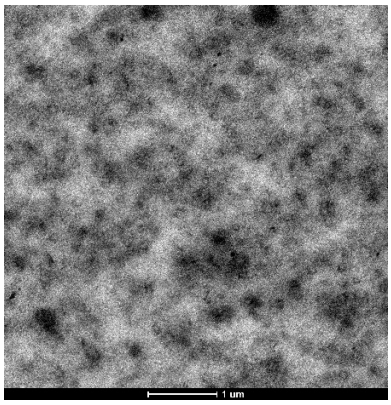
(Scale bar: 1 µm)	(Scale bar: 1 µm)	(Scale bar: 1 µm)

Figure 9: TEM pictures of cryo-microtome cuts of the cast films made from hybrids of different architectures (20wt.% PHU, room temperature, 55% relative humidity). No staining was performed and the phase contrast is only due to the latex composition. The dark phase was identified as the poly(hydroxyurethane).

Figure 10 presents the stress-strain curves obtained in tensile experiments. Latexes containing multi-functionalized PHUs formed films prone to crack likely because the casting temperature (30 ºC) was close to the MFFT (27 ºC) and the films cast for the tensile tests were thicker than the film prepared for the MFFT test. Thicker films tend to crack easier than thin films because the stresses created during film formation are greater in thicker films.[45] The mechanical properties are listed in Table 5. It can be seen that incorporation of PHU into the poly(butyl methacrylate – *co* – stearyl acrylate) (P(BMA-*co*-SA)) chains initially reduced the stiffness of the P(BMA-*co*-SA) initially lowering the Young's modulus. The formation of crosslinks in the multifunctionalized PHU counteracted the softening effect of the PHU leading to a clear increase of the Young's modulus. A similar trend was found for the stress at break. The strain at break showed the opposite behavior with the longest one corresponding to the softest bi-functional PHU containing latex. The toughness, which represents the compromise between stress and

strain at break, was maximum for bi-functional PHU-containing latex. It is worth pointing out that the wetting agent acted as a plasticizer (Figure S5).

It can be concluded that grafting enabled fine tuning of the mechanical properties of the PHU containing hybrids and that a mild incorporation of the PHU into the P(BMA-*co*-SA) chains led to tougher coatings, whereas crosslinking increased the stiffness of the films.

Clearly, the present approach is not limited to the (meth)acrylic monomers used in this work, opening the way to access materials for different end-uses (*e.g.* adhesives of low T_g and coatings with even higher T_g).

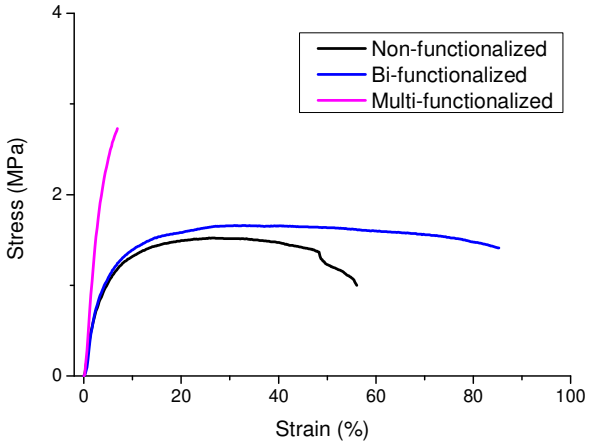

Figure 10: Stress-strain curves of the cast films (30°C, 55% humidity 1wt% wetting agent)

Table 5: Tensile test results of the cast films. The films were cast at 30°C, 55% humidity with 1wt% of wetting agent.

Temperature [°C]	Architecture	Young Modulus [MPa]	Strain at break [%]	Stress at break [MPa]	Toughness [MPa]
30	Non-funct.	52 ± 11	41.4 ± 6.1	1.5 ± 0.05	0.63 ± 0.10
30	Bi-funct.	46 ± 11	76.2 ± 9.2	1.3 ± 0.4	1.14 ± 0.15
30	Multi-funct.	86 ± 20	5.2 ± 4.0	2.2 ± 0.7	0.09 ± 0.07

4. Conclusions

In this study, waterborne isocyanate free grafted poly(hydroxy urethane)-poly(meth)acrylate (PHU-PMA) hybrid dispersions were synthesized and the effect of grafting on the particle and film morphologies as well as on the mechanical properties of the films was investigated. The dispersions were prepared by free radical polymerization of a miniemulsion in which the organic phase was a mixture of methacrylate functionalized PHU, BMA and SA. TBHP/AsAc was used as a redox pair. Functionalized PHUs with different architectures were prepared. Bi-functional PHUs were synthesized by reacting amine terminated PHUs with mono-carbonated glycidyl methacrylate (monoCC-GMA). A functionalized PHU having multiple methacrylic groups in the backbone was also prepared by reacting the OH groups of the PHU with methacrylic anhydride. A non-functionalized hybrid was prepared for comparative purposes.

The structure of the functionalized PHU had a substantial effect on the polymer hybrid. All hybrids presented two T_gs, one at about 26-27 °C that corresponded to the (meth)acrylic polymer and another one at a lower temperature for the PHU. This lower temperature increased from -20 °C for the hybrid containing non-functionalized to -12°C for the hybrid prepared with the multi-functionalized PHU, which indicates that grafting increased with the methacrylic functionalization. Functionalization had also a strong effect on the molar mass distribution. AF4 measurements showed that the non-functionalized and the bi-functional (methacrylate-terminated) hybrids presented two peaks, the small one corresponding to the ungrafted PHU and the large one to the poly(butyl methacrylate – *co* – stearyl acrylate) that included the PHU grafted. This result was expected for the non-functionalized PHU, but is was surprising for the bi-functionalized PHU, because it indicates that some PHUs were not functionalized or were not

reactive enough. The multifunctionalized hybrid presented a single peak. Functionalized hybrids yielded macroscopic gel. Clear films were cast from all the hybrids, although that of the multifunctional PHU was prone to crack. For the functionalized PHUs, the minimum film forming temperature (MFFT) increased with the crosslinking density.

The incorporation of some PHU into the P(BMA-*co*-SA) chains reduced the stiffness of the P(BMA-*co*-SA) initially lowering the Young's modulus and stress at break and increasing the strain at break and toughness. Higher incorporation of PHU led to the formation of crosslinks that counteracted the softening effect of the PHU leading to a clear increase of the Young's modulus and stress at break, but a lower strain at break and toughness was obtained.

The results presented in this article show that grafting enabled a fine tuning of the mechanical properties of the PHU containing hybrids, with an increased stiffness of the films with the crosslinking density. Using other (meth)acrylic monomers, this approach opens the possibility to access materials with widely different end-uses.

AUTHOR INFORMATION

Corresponding Authors

* Henri Cramail - cramail@enscbp.fr

* José M. Asua – jm.asua@ehu.eus

Author Contributions

The manuscript was written through contributions of all authors. All authors have given approval to the final version of the manuscript.

Notes

The authors declare that they have no known competing financial interests or personal relationships that could have appeared to influence the work reported in this paper.

ACKNOWLEDGMENT

BB acknowledges both the University of Bordeaux (UB) as well as POLYMAT for funding. From the UB side, this project has benefited from state funding, managed by the French National Research Agency (ANR). The funding is allocated in the framework of the "Investments for the Future" program, with the reference number ANR - n ° ANR-10-IDEX-03-02.

REFERENCES

[1] K.I. Winey, R.A. Vaia, Polymer Nanocomposites, MRS Bull. 32 (2007) 314–322. https://doi.org/DOI: 10.1557/mrs2007.229.

[2] B.M. Novak, Hybrid Nanocomposite Materials between inorganic glasses and organic polymers, Adv. Mater. 5 (1993) 422–433. https://doi.org/10.1002/adma.19930050603.

[3] S.C. Thickett, G.H. Teo, Recent advances in colloidal nanocomposite design: Via heterogeneous polymerization techniques, Polym. Chem. 10 (2019) 2906–2924. https://doi.org/10.1039/c9py00097f.

[4] A. Guyot, K. Landfester, F. Joseph Schork, C. Wang, Hybrid polymer latexes, Prog. Polym. Sci. 32 (2007) 1439–1461. https://doi.org/10.1016/j.progpolymsci.2007.07.003.

[5] S. Mehravar, N. Ballard, R. Tomovska, J.M. Asua, Polyurethane/Acrylic Hybrid Waterborne Dispersions: Synthesis, Properties and Applications, Ind. Eng. Chem. Res. 58 (2019) 20902–20922. https://doi.org/10.1021/acs.iecr.9b02324.

[6] W. Friederichs, Introduction, Basic Reaction, Starting Materials, Structure and Morphology, and Production in Chapter "Polyurethane," in: Ullmann's Encycl. Ind. Chem., 7th edition, Wiley-VCH Verlag GmbH & Co. KGaA., 2005. https://doi.org/10.1002/14356007.a21_665.pub2.

[7] I. Yilgör, E. Yilgör, G.L. Wilkes, Critical parameters in designing segmented polyurethanes and their effect on morphology and properties: A comprehensive review, Polymer (Guildf). 58 (2015) A1–A36. https://doi.org/10.1016/j.polymer.2014.12.014.

[8] P. Król, Synthesis methods, chemical structures and phase structures of linear polyurethanes. Properties and applications of linear polyurethanes in polyurethane elastomers, copolymers and ionomers, Prog. Mater. Sci. 52 (2007) 915–1015. https://doi.org/10.1016/j.pmatsci.2006.11.001.

[9] B.K. Kim, J.C. Lee, Modification of waterborne polyurethanes by acrylate incorporations, J. Appl. Polym.

Sci. 58 (1995) 1117–1124. https://doi.org/10.1002/app.1995.070580705.

[10] Y. Okamoto, Y. Hasegawa, F. Yoshino, Urethane/ acrylic composite polymer emulsions, Prog. Org. Coatings. 29 (1996) 175–82.

[11] H.L. Manock, New developments in polyurethane and PU/acrylic dispersions, Pigment Resin Technol. 29 (2000) 143–151. https://doi.org/10.1108/03699420010334295.

[12] A. Lopez, E. Degrandi-Contraires, E. Canetta, C. Creton, J.L. Keddie, J.M. Asua, Waterborne polyurethane-acrylic hybrid nanoparticles by miniemulsion polymerization: Applications in pressure-sensitive adhesives, Langmuir. 27 (2011) 3878–3888. https://doi.org/10.1021/la104830u.

[13] R. Udagama, E. Degrandi-Contraires, C. Creton, C. Graillat, T.F.L. McKenna, E. Bourgeat-Lami, Synthesis of acrylic-polyurethane hybrid latexes by miniemulsion polymerization and their pressure-sensitive adhesive applications, Macromolecules. 44 (2011). https://doi.org/10.1021/ma200073d.

[14] E. Degrandi-Contraires, R. Udagama, E. Bourgeat-Lami, T. McKenna, K. Ouzineb, C. Creton, Mechanical properties of adhesive films obtained from PU-acrylic hybrid particles, Macromolecules. (2011). https://doi.org/10.1021/ma2000702.

[15] V. Daniloska, P. Carretero, R. Tomovska, J.M. Asua, High performance pressure sensitive adhesives by miniemulsion photopolymerization in a continuous tubular reactor, Polymer (Guildf). 55 (2014) 5050–5056. https://doi.org/10.1016/j.polymer.2014.08.038.

[16] S. Mehravar, N. Ballard, A. Agirre, R. Tomovska, J.M. Asua, Role of Grafting on Particle and Film Morphology and Film Properties of Zero VOC Polyurethane/Poly(meth)acrylate Hybrid Dispersions, Macromol. Mater. Eng. 304 (2019) 1800532. https://doi.org/10.1002/mame.201800532.

[17] S. Mehravar, K.J. Roschmann, P.U. Arocha, B. Reck, A. Agirre, R. Tomovska, J.M. Asua, N. Ballard, Correlating microstructure and performance of PU/(meth)acrylic hybrids as hardwood floor coating, Prog. Org. Coatings. 131 (2019) 417–426. https://doi.org/10.1016/j.porgcoat.2019.03.002.

[18] D. Kukanja, J. Golob, A. Zupancic-Valant, M. Krajnc, The structure and properties of acrylic-polyurethane hybrid emulsions and comparison with physical blends, J. Appl. Polym. Sci. 78 (2000) 67–80. https://doi.org/10.1002/1097-4628(20001003)78:1<67::AID-APP100>3.0.CO;2-4.

[19] L. Wu, B. You, D. Li, Synthesis and characterization of urethane/acrylate composite latex, J. Appl. Polym. Sci. 84 (2002) 1620–1628. https://doi.org/10.1002/app.10526.

[20] S. Chen, L. Chen, Structure and properties of polyurethane/polyacrylate latex interpenetrating networks hybrid emulsions, Colloid Polym. Sci. 282 (2003) 14–20. https://doi.org/10.1007/s00396-003-0863-8.

[21] R.A. Brown, R.G. Coogan, D.G. Fortier, M.S. Reeve, J.D. Rega, Comparing and contrasting the properties of urethane/acrylic hybrids with those of corresponding blends of urethane dispersions and acrylic emulsions, in: Prog. Org. Coatings, Elsevier, 2005: pp. 73–84. https://doi.org/10.1016/j.porgcoat.2004.03.009.

[22] C. Wang, F. Chu, C. Graillat, A. Guyot, C. Gauthier, J.P. Chapel, Hybrid polymer latexes: Acrylics-polyurethane from miniemulsion polymerization: Properties of hybrid latexes versus blends, in: Polymer (Guildf)., Elsevier BV, 2005: pp. 1113–1124. https://doi.org/10.1016/j.polymer.2004.11.051.

[23] C. Wang, F. Chu, C. Graillat, A. Guyot, C. Gauthier, Hybrid polymer latexes - Acrylics-polyurethane: II. Mechanical properties, Polym. Adv. Technol. 16 (2005) 139–145. https://doi.org/10.1002/pat.557.

[24] C.Y. Li, W.Y. Chiu, T.M. Don, Morphology of PU/PMMA hybrid particles from miniemulsion polymerization: Thermodynamic considerations, J. Polym. Sci. Part A Polym. Chem. 45 (2007) 3359–3369. https://doi.org/10.1002/pola.22086.

[25] M. Hirose, F. Kadowaki, J. Zhou, The structure and properties of core-shell type acrylic-polyurethane hybrid aqueous emulsions, Prog. Org. Coatings. 31 (1997) 157–169. https://doi.org/10.1016/S0300-9440(97)00032-5.

[26] V.D. Athawale, M.A. Kulkarni, Preparation and properties of urethane/acrylate composite by emulsion polymerization technique, Prog. Org. Coatings. 65 (2009) 392–400. https://doi.org/10.1016/j.porgcoat.2009.03.004.

[27] S.J. Son, K.B. Kim, Y.H. Lee, D.J. Lee, H. Do Kim, Effect of acrylic monomer content on the properties of waterborne poly(urethane-urea)/acrylic hybrid materials, J. Appl. Polym. Sci. 124 (2012) 5113–5121. https://doi.org/10.1002/app.35662.

[28] U. Šebenik, M. Krajnc, Properties of acrylic-polyurethane hybrid emulsions synthesized by the semibatch emulsion copolymerization of acrylates using different polyurethane particles, J. Polym. Sci. Part A Polym. Chem. 43 (2005) 4050–4069. https://doi.org/10.1002/pola.20896.

[29] A. Dong, Y. An, S. Feng, D. Sun, Preparation and morphology studies of core-shell type waterborne polyacrylate-polyurethane microspheres, J. Colloid Interface Sci. 214 (1999) 118–122. https://doi.org/10.1006/jcis.1999.5847.

[30] B. Bizet, É. Grau, H. Cramail, J.M. Asua, Water-based non-isocyanate polyurethane-ureas (NIPUUs), Polym. Chem. 11 (2020) 3786–3799. https://doi.org/10.1039/D0PY00427H.

[31] L. Meng, X. Wang, M. Ocepek, M.D. Soucek, A new class of non-isocyanate urethane methacrylates for the urethane latexes, Polymer (Guildf). 109 (2017) 146–159. https://doi.org/10.1016/j.polymer.2016.12.022.

[32] L. Meng, M.D. Soucek, Z. Li, T. Miyoshi, Investigation of a non-isocyanate urethane functional monomer in latexes by emulsion polymerization, Polymer (Guildf). 119 (2017) 83–97. https://doi.org/10.1016/j.polymer.2017.05.006.

[33] Z. Ma, C. Li, H. Fan, J. Wan, Y. Luo, B.G. Li, Polyhydroxyurethanes (PHUs) Derived from Diphenolic Acid and Carbon Dioxide and Their Application in Solvent- and Water-Borne PHU Coatings, Ind. Eng. Chem. Res. 56 (2017) 14089–14100. https://doi.org/10.1021/acs.iecr.7b04029.

[34] C. Zhang, H. Wang, Q. Zhou, Waterborne isocyanate-free polyurethane epoxy hybrid coatings synthesized from sustainable fatty acid diamine, Green Chem. 22 (2020) 1329–1337. https://doi.org/10.1039/C9GC03335A.

[35] B. Bizet, E. Grau, H. Cramail, J.M. Asua, Volatile Organic Compound-Free Synthesis of Waterborne Poly(hydroxy urethane)–(Meth)acrylic Hybrids by Miniemulsion Polymerization, ACS Appl. Polym. Mater. 2 (2020) 4016–4025. https://doi.org/10.1021/acsapm.0c00657.

[36] C. Wang, F. Chu, L. Jin, M. Lin, Y. Xu, A. Guyot, Polyurethane-acrylate hybrid latexes from miniemulsion polymerization: effect of endgroups on structure and properties, Polym. Adv. Technol. 20 (2009) 319–326. https://doi.org/10.1002/pat.1270.

[37] S. Mehravar, N. Ballard, R. Tomovska, J.M. Asua, The Influence of Macromolecular Structure and Composition on Mechanical Properties of Films Cast from Solvent-Free Polyurethane/Acrylic Hybrid Dispersions, Macromol. Mater. Eng. 304 (2019) 1900155.

https://doi.org/10.1002/mame.201900155.

[38] M. Manea, A. Chemtob, M. Paulis, J.C. de la Cal, M.J. Barandiaran, J.M. Asua, Miniemulsification in high-pressure homogenizers, AIChE J. 54 (2008) 289–297. https://doi.org/10.1002/aic.11367.

[39] J.M. Asua, Challenges for industrialization of miniemulsion polymerization, Prog. Polym. Sci. 39 (2014) 1797–1826. https://doi.org/10.1016/j.progpolymsci.2014.02.009.

[40] M.A. Taylor, Synthesis of Polymer Dispersions, in: Polym. Dispersions Their Ind. Appl., Wiley-VCH Verlag GmbH & Co. KGaA, 2003: pp. 15–40. https://doi.org/10.1002/3527600582.ch2.

[41] S. Podzimek, Light Scattering, Size Exclusion Chromatography and Asymmetric Flow Field Flow Fractionation: Powerful Tools for the Characterization of Polymers, Proteins and Nanoparticles, John Wiley and Sons, 2011. https://doi.org/10.1002/9780470877975.

[42] V. Schimpf, A. Asmacher, A. Fuchs, B. Bruchmann, R. Mülhaupt, Polyfunctional Acrylic Nn-isocyanate Hydroxyurethanes as Photocurable Thermosets for 3D Printing, Macromolecules. (2019) acs.macromol.9b00330. https://doi.org/10.1021/acs.macromol.9b00330.

[43] W. Wang, A.N. Nikitin, R.A. Hutchinson, Consideration of Macromonomer Reactions in *n* -Butyl Acrylate Free Radical Polymerization, Macromol. Rapid Commun. 30 (2009) 2022–2027. https://doi.org/10.1002/marc.200900445.

[44] A.-M. Zorn, T. Junkers, C. Barner-Kowollik, A Detailed Investigation of the Free Radical Copolymerization Behavior of *n* -Butyl Acrylate Macromonomers, Macromolecules. 44 (2011) 6691–6700. https://doi.org/10.1021/ma201345m.

[45] M.S. Tirumkudulu, W.B. Russel, Cracking in Drying Latex Films, Langmuir. 21 (2005) 4938–4948. https://doi.org/10.1021/la048298k.

TABLE OF CONTENT – Graphical Abstract

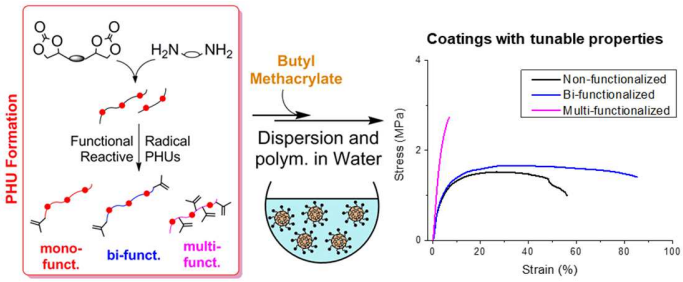

For table of content use only